Combined effect of tumor necrosis factor-related apoptosis-inducing ligand and ionizing radiation in breast cancer therapy

Arul M. Chinnaiyan*†‡, Uttara Prasad*§, Sunita Shankar*†, Daniel A. Hamstra*§, Murthy Shanaiah*§, Thomas L. Chenevert*¶, Brian D. Ross*¶‖, and Alnawaz Rehemtulla*‡§**

*Center for Molecular Imaging and Departments of †Pathology, §Radiation Oncology, ¶Radiology, and ‖Biochemistry, University of Michigan Medical School, 1301 Catherine Road, MSI Room 4237, Ann Arbor, MI 48109-0602

Tumor necrosis factor-related apoptosis-inducing ligand (TRAIL) is a potent endogenous activator of the cell death pathway and functions by activating the cell surface death receptors 4 and 5 (DR4 and DR5). TRAIL is nontoxic *in vivo* and preferentially kills neoplastically transformed cells over normal cells by an undefined mechanism. Radiotherapy is a common treatment for breast cancer as well as many other cancers. Here we demonstrate that ionizing radiation can sensitize breast carcinoma cells to TRAIL-induced apoptosis. This synergistic effect is p53-dependent and may be the result of radiation-induced up-regulation of the TRAIL-receptor DR5. Importantly, TRAIL and ionizing radiation have a synergistic effect in the regression of established breast cancer xenografts. Changes in tumor cellularity and extracellular space were monitored *in vivo* by diffusion-weighted magnetic resonance imaging (diffusion MRI), a noninvasive technique to produce quantitative images of the apparent mobility of water within a tissue. Increased water mobility was observed in combined TRAIL- and radiation-treated tumors but not in tumors treated with TRAIL or radiation alone. Histological analysis confirmed the loss of cellularity and increased numbers of apoptotic cells in TRAIL- and radiation-treated tumors. Taken together, our results provide support for combining radiation with TRAIL to improve tumor eradication and suggest that efficacy of apoptosis-inducing cancer therapies may be monitored noninvasively, using diffusion MRI.

Breast cancer continues to be a major health problem worldwide despite recent advances in its diagnosis and treatment (1). Novel cytotoxic and hormonal agents have emerged from an improved understanding of oncogenesis and the biology of the mammary gland. Ionizing radiation is an important treatment modality for breast cancer as well as many other cancers (1). As an integral part of breast-conserving treatment, radiotherapy reduces the incidence of local and regional recurrences. Ionizing radiation can damage cells directly by interacting with critical cellular targets or indirectly by generating free radicals (2). Regardless of the mechanism, radiation-induced damage often triggers the endogenous suicide machinery of cells (3, 4).

Tumor necrosis factor-related apoptosis-inducing ligand (TRAIL) (also known as APO-2L) is an apoptosis-inducing member of the tumor necrosis factor (TNF) gene family that includes TNF, CD95 Ligand (CD95L), and lymphotoxin-α (LT-α), among others. TNF family members are homotrimeric molecules that function by interacting with, trimerizing, and thus activating their respective cell-surface receptors. A subset of these type II transmembrane proteins activate the cell death pathway (5, 6). They transduce the apoptotic signal by engaging death receptors that belong to a subfamily of the TNF receptor gene superfamily and include TNFR1, CD95, death receptor (DR3), DR4, DR5, and DR6 (6). One of the prototypic and best-characterized death receptor–death ligand pairs is CD95 and CD95L (also known as the Fas/APO-1 system) (7, 8).

In the CD95 pathway, ligand-induced activation of the receptor causes recruitment of the intracellular death adapter molecule FADD (Fas-associated death domain protein) (9, 10), which can then engage the death protease caspase 8 (11, 12). By facilitating the proximity of zymogen molecules, FADD triggers caspase 8 autoactivation, hierarchically controlling the activation of downstream caspases and ultimately manifesting in the apoptotic phenotype (13). In an analogous fashion, TRAIL binds to the death receptors DR4 and DR5 (14, 15). Homologs of the FADD–caspase 8 axis likely dictate the suicide response emanating from DR4 and DR5 (14). Interestingly, TRAIL also binds DcR1 (decoy receptor 1) and DcR2, two related decoy receptors that fail to signal cell death (14–17). Functionally, TRAIL has been shown to preferentially kill transformed cell lines over normal cells (18). Various theories have emerged to explain this discrepancy, including differential expression levels of death receptors, decoy receptors, and death inhibitors (19).

Although TNF and CD95L induce apoptosis of cancer cells, systemic administration of either agent is toxic to mice. Because of its ability to activate the proinflammatory transcription factor NF-κB, TNF infusion causes a lethal septic-shock like state in mice (20, 21). Activation of the CD95 pathway *in vivo* causes massive liver damage consequent to CD95-mediated hepatocyte apoptosis (22, 23). Unlike TNF and CD95L, TRAIL is nontoxic systemically, enhancing its potential as a cancer therapeutic (18). Recent studies have shown that systemic administration of TRAIL can slow the growth and, in some cases, induce regression of tumor cell xenografts (18, 24). TRAIL, as a selective killer of tumor cells, has also received considerable press (25) and is currently in preclinical trials.

Ionizing radiation continues to have an important role in cancer treatment. Identifying biological compounds that will enhance the efficacy of radiotherapy is of tremendous interest, especially because of the existence of many radioresistant tumors. Previous studies have shown that angiostatin, an inhibitor of angiogenesis, has a combined antitumor effect with radiation (26). Here we show that an endogenous activator of the apoptosis pathway, TRAIL, can work in concert with radiation to eradicate breast cancer tumors. Unlike radiotherapy, TRAIL functions systemically and thus has the added benefit of targeting metastases. The molecular mechanism of the combined antitumor activity of TRAIL and radiation was also investigated.

In this study, tumor therapy is monitored noninvasively by using diffusion-weighted MRI, a sensitive imaging modality that can detect alterations in extracellular water mobility. The diffusion of water in tissue is strongly affected by fluid viscosity and membrane permeability between intra- and extracellular compartments, active transport and flow, and directionality of structures that impede or enhance mobility. As cells are damaged and killed by therapeutic interventions, the integrity of cell membranes may be compromised and the fractional volume of the interstitial space may increase because of apoptotic body formation and cell loss. These changes are expected to increase the mobility of water in the damaged tissue. Mobility of tissue water *in vivo* can be noninvasively quantified as an apparent diffusion coefficient (ADC) by using diffusion MRI (27). Detection of changes in the microscopic water environment by quanitative diffusion MRI may serve as a "window" to observe apoptotic activity *in vivo*. The ability to monitor apoptosis-inducing cancer therapy noninvasively should aid assessment of therapeutic efficacy and treatment stratification on an individual basis.

Materials and Methods

Preparation of Recombinant TRAIL. The expression construct used to produce TRAIL was described elsewhere (pet 15b-HIS-TRAIL) (28). Polyhistidine-tagged TRAIL was purified from *Escherichia coli* by using standard nickel affinity chromatography as per the manufacturer (Qiagen, Chatsworth, CA). Preparations were made endotoxin-free by sequential detergent extraction (Triton X-114) (29, 30). Detergent was removed from the final preparation by using Bio-Rad SM-2 beads (30). Endotoxin testing was done by using the Limulus Amebocyte Lysate Assay (BioWhittaker) (30).

Cell Lines. The SUM cell lines are described in a web page maintained by S. Ethier at the University of Michigan Cancer Center (http://p53.cancer.med.umich.edu/umbnkdb.html). The breast carcinoma cell line MCF7 was grown in RPMI 1640 complete medium [10% heat-inactivated fetal bovine serum (HyClone), L-glutamine, penicillin/streptomycin, and non-essential amino acids]. MCF7-vector and p53-DN cells lines were described previously (31).

Apoptosis/Cell Death Assays. To assess nuclear morphology, fluorescent DNA-staining dyes were used as described (32). In brief, MCF7 cells were fixed in 100% ice-cold methanol and were incubated at −20°C for 10 min. They were then washed three times in PBS and were stained at room temperature for 10 min in a 100 μg/ml solution of propidium iodide (Sigma) made in PBS. The suspended cells were mounted onto glass slides by using Vectashield mounting medium (Vector Laboratories). The propidium iodide-stained cells were visualized by fluorescence microscopy using a FITC barrier filter cube. Flow cytometry for sub-GI content was done as described (33). To assess cell viability, the MTS [3-(4, 5-dimethylthiazol-2yl)-5-(3carboxymethoxyphentyl)-2-(4-sulfophenyl)-2H-tetrazolium] conversion assay was done on the indicated cell lines according to the manufacturer's specifications (Promega). In brief, MTS was added to cells cultured in a 96-well format and was incubated for 1–3 hr, and absorbance was measured by spectrophotometry.

DNA fragmentation [terminal deoxynucleotide transferase-mediated dUTP-biotin nick-end labeling (TUNEL) staining] was determined by using the ApopTag kit and was performed according to the manufacturer's conditions (Intergen, Purchase, NY). The TUNEL-stained cells were counterstained with propidium iodide (10 μg/ml), and the tissue sections were visualized by fluorescence microscopy.

Immunoblotting. MCF7 cells (5×10^6) were harvested at the indicated times after irradiation. Cells were pelleted, freeze-thawed once, and lysed in 1.0% Nonidet P-40 for 10 min. Samples were centrifuged at $12,000 \times g$ for 25 min at 4°C. Cytosolic extracts were removed and added to sample buffer. Samples were separated by 10% SDS/PAGE and were transferred to nitrocellulose. Immunoblotting for DR4 was done by using a rabbit polyclonal Ab (Upstate Biotechnology, Lake Placid, NY) at 0.5 μg/ml. DR5 was immunoblotted by using a goat polyclonal Ab (Alexis, San Diego) at 1 μg/ml. Appropriate horseradish peroxidase-conjugated secondary antibodies (GIBCO/BRL) were used, and the blots developed were by ECL (Amersham).

***In Vivo* Model.** Animal experiments, including designations for survival outcomes, were approved by the University of Michigan Committee on Use and Care of Animals. MCF7 human breast carcinoma tumors were established in female NIH III nude mice (6–8 weeks, Charles River Breeding Laboratories) by serial subcutaneous transplantation of tumor fragments bilaterally between the fourth and fifth mammary fat pads using a 12-gauge trochar. At the time of transplantation, mice were also implanted subcutaneously on the dorsal surface with a 0.72-mg 17-β-estradiol tablet (Innovative Research of America). Tumors were measured 2–3 times per week in two dimensions by using calipers, and the volumes were calculated by using the formula, volume = [(length $\times$ (width)^2) $\times$ π/6]. Treatment was initiated when the tumors reached a mean volume of 150 mm^3.

Mouse tumor irradiation was performed by using a Theratron 80 ^{60}Co with a dose rate of 85 cGy per minute for a focus-to-skin distance of 80 cm. Radiation was delivered in 3 fractions of 5 Gy each, which were administered on days 1, 3, and 5. Mice were placed in a custom designed restraint apparatus in the lateral decubitous position, and the tumors were irradiated with a horizontal field. The remaining parts of their bodies were shielded by a cerrobend block of 7-cm thickness. Thermoluminescnese dosimeter placed behind the cerrobend measured 3% of the dose at the central ray of the treatment field. Starting on day 3, mice received saline or recombinant TRAIL (5 mg/kg i.p.) daily for 7 days either alone or in combination with radiotherapy. Mice were weighed every 2–3 days. Values for tumor volumes represent the mean $\pm$ the standard error of the mean.

Diffusion Magnetic Resonance Imaging. Imaging was performed before and after 7 days of treatment on a Varian Unity Inova system equipped with a 7.0-tesla, 18.3-cm horizontal bore magnet and a quadrature bird cage design coil (USA Instruments, Aurora, IL). For MRI examination, mice were anesthetized with an isofluorane/air mixture and were maintained at 37°C inside the magnet by using a heated, thermostated circulating water bath. A single-slice sagittal spin-echo sequence was used to confirm proper animal positioning and to prescribe subsequent imaging. An isotropic, diffusion-weighted sequence (34) was used with two interleaved b-factors (Δb = 1,148 s/mm^2) and the following acquisition parameters: repetition time/echo time = 3,500/60 ms, 128 $\times$ 128 matrix, and a 3-cm field of view. Thirteen 1-mm-thick slices separated by a 0.2-mm gap were used to cover the entire tumor. The z-gradient first moment was zeroed to reduce the dominant source of motion artifact. To further reduce motion artifact, a 32-point navigator echo was prepended to each phase-encode echo. The phase deviation of each navigator echo relative to their mean was subtracted from the respective image echoes before the phase-encoded Fourier transform. Isotropic ADC maps were calculated for each image set acquired before treatment and at 7 days after treatment initiation.
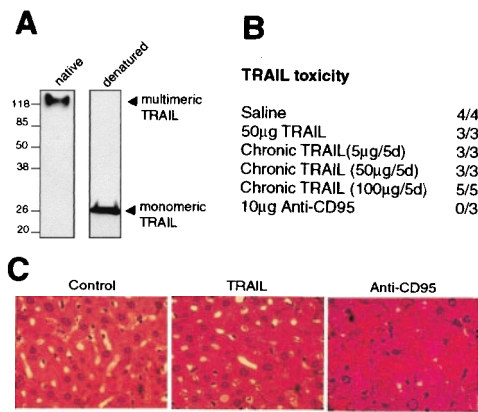
Fig. 1. Polyhistidine-tagged recombinant TRAIL is nontoxic to mice. (*A*) TRAIL was run on a native SDS/PAGE gel (*Left*) or under reduced, denaturing conditions (*Right*). Monomeric TRAIL runs at ≈27 kDa whereas multimeric TRAIL runs at ≈120 kDa. (*B*) His-tagged TRAIL is nontoxic to NIH III nude mice. Mice were injected intravenously with saline, 50 μg of TRAIL, or 10 μg of Jo2 mAb (anti-CD95, PharMingen) once. Alternatively, mice were treated with daily injections of 5, 50, or 100 μg of TRAIL for 5 consecutive days (Chronic TRAIL). Mice were weighed 2–3 times per week with no significant decreases in control or TRAIL-treated mice (data not shown). Mice treated with Jo2 mAb died within 3 hr of injection whereas control or TRAIL-treated mice survived past 45 days. Ratios represent the number of mice that survived past 45 days over the total number treated. (*C*) Liver pathology of TRAIL-treated mice. Livers were isolated and sectioned in control mice and TRAIL treated mice 45 days after treatment whereas anti-CD95 livers were isolated 2 hr after injection of Jo2 mAb. Tissue sections were hematoxylin- and eosin-stained. TRAIL treatment chronically (for 45 days) or acutely (for 2 hr, data not shown) did not alter liver histology as compared with the control. However, activation of the CD95 pathway induced massive hepatocyte cell death (as evidenced by the numerous apoptotic figures), hemorrhage, and other alterations in morphology.

Results

Recombinant TRAIL Is a Multimer That Has Apoptotic Activity Against Breast Carcinoma Cells but Not Normal Breast Epithelial Cells. TRAIL, like other members of the TNF family, functions as a trimer to aggregate specific death receptors on the surface of cells. Previous studies have used TRAIL, expressed in mammalian cells, and N-terminally fused with a leucine zipper motif to facilitate oligomerization. In this study, we generated large amounts of recombinant TRAIL in *E. coli*, N-terminally fused with a polyhistidine tag. Under native, nondenaturing conditions, our TRAIL preparation migrates as a multimeric complex of ≈120 kDa (Fig. 1*A*). By contrast, under reduced, denaturing conditions, TRAIL resolves on SDS/PAGE as a 27-kDa monomer (Fig. 1*A*).

The apoptotic activity of TRAIL was tested against a panel of cell lines (Table 1). TRAIL exposure induced apoptosis in most breast carcinoma cell lines but not normal human mammary epithelial cells. SUM 149, SUM 229, and MCF10A breast carcinoma cell lines were especially sensitive to TRAIL-induced apoptosis, dying within 3 hr of TRAIL exposure (>90% cell death). The SUM cell lines are human breast tumor cells freshly isolated and characterized by S. Ethier at the University of Michigan. These lines are maintained under defined growth factor conditions and have been characterized for genetic alterations (http://p53.cancer.med.umich.edu/umbnkdb. html). Other non-breast cancer cell lines tested were also differentially sensitive to TRAIL-induced apoptosis (Table 1).

Multimeric TRAIL Is Nontoxic *in Vivo*. Infusion of TNF or antibody to CD95 has been shown to be lethal to mice consequent to activation of the endogenous NF-κB or apoptotic pathway, respectively. To determine *in vivo* toxicity, intravenous injections

Table 1. Sensitivity of various human cell lines to TRAIL-induced apoptosis

Breast cell lines	
SUM149	+ + + + + +
SUM229	+ + + + + +
MCF10A	+ + + + +
SUM102	+ + + +
SUM44	+
MCF7	+
SUM185	+
SUM131/5MD2	+
SUM52	+
SUM225	+
SUM190	−
Normal HME	−
Other cell lines	
HT29 (colon cancer)	+
A549 (lung cancer)	−
UMSCCVI (squamous cancer)	+ +
293T	−
HCT 116 ( )	+ +
Glial U251	+ + + + +
DU145 (prostate cancer)	+

Cell lines were assessed for apoptosis based on morphologic criteria. Relative apoptosis is represented whereby 6+ equals >95% apoptosis after overnight incubation with saturating doses of TRAIL (1,000 ng/ml). 3+ equals ∼50% apoptosis. 1+ equals approximately 10% apoptosis, and − represents virtually complete resistance to TRAIL.

of His-tagged TRAIL were done in NIH III nude mice. Animals injected once with saline or 50 μg of TRAIL exhibited no observable deleterious effects (e.g., decrease in survival, weight loss or liver pathology), and all survived past 45 days (Fig. 1*B*). Furthermore, mice treated with daily injections of 5, 50, or 100 μg of TRAIL for 5 days similarly exhibited no toxicity past 45 days. By contrast, activation of the CD95 pathway by a single injection of the Jo2 agonist antibody caused the mice to become moribund within 1–2 hr, and all were dead by 3 hr. Unlike saline or TRAIL-treated mice, livers of anti-CD95 treated mice showed significant hepatocellular degeneration, hemorrhage, and necrosis (Fig. 1*C*).

TRAIL and Ionizing Radiation Have a Synergistic Apoptotic Effect On Breast Cancer Cell Lines *in Vitro*. We next assessed whether radiation and TRAIL have a greater than additive apoptotic activity *in vitro*. To address this question effectively, we chose a cell line that has low sensitivity to TRAIL, the MCF7 breast carcinoma cell line (Table 1). Although TRAIL and 8-Gy radiation induced ≈10% apoptosis alone, together they had a synergistic effect *in vitro*—causing ≈40% apoptosis as assessed by morphology and sub-G_1 DNA content (Fig. 2*A*). Next, we tested various breast carcinoma cell lines from our initial panel (Table 1). Like MCF7 cells, SUM44 cells also showed an enhanced apoptotic effect when TRAIL and radiation were combined (≈15% cell death with each treatment alone and 40% cell death with combined treatment) (Fig. 2*B*). However, SUM149, SUM225, and SUM190 cells did not exhibit a synergistic apoptotic response when TRAIL and radiation were combined (Fig. 2 *C* and *D*). Interestingly, we noticed a correlation between TRAIL/radiation synergy and the p53 status of the cell lines. Cells expressing wild-type p53 (MCF7, SUM44) exhibited a synergistic response to TRAIL and radiation whereas those that are p53 mutants (SUM149, SUM225, and SUM190) did not.

The Synergistic Effect of TRAIL and Ionizing Radiation Is p53-Dependent and May Be Mediated by Up-Regulation of DR5. To provide a mechanistic basis for the synergy between TRAIL and radiation,
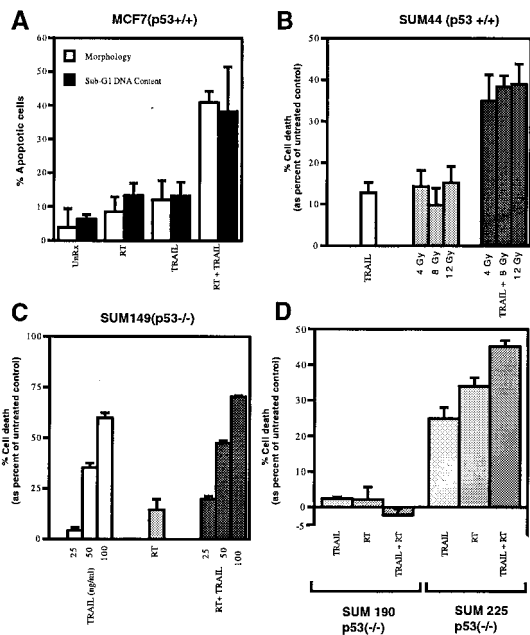
Chinnaiyan *et al.*

www.manaraa.com

Fig. 2. TRAIL and radiation have a combined apoptotic effect in p53 wild-type breast carcinoma cells. (*A*) MCF7 cells (p53 wild-type) were treated with 8 Gy radiotherapy (RT) or TRAIL (1,000 ng/ml) alone or in combination. Apoptosis was assessed 42 hr posttreatment by morphology (DNA staining) or sub-G_1 DNA content (flow cytometry). UnRx, untreated control. (*B*) SUM44 cells (p53 wild-type) were treated with TRAIL and selected doses of RT alone or in combination for 42 hr, and cell death was assessed by MTS assay. Cell death was determined relative to the percent viable cells in the untreated control. (*C*) SUM 149 cells (p53 mutant) were treated with 8 Gy RT and selected doses of TRAIL alone or in combination, and cell death was assessed by MTS assay 42 hr posttreatment. (*D*) SUM 190 (p53 mutant) and SUM225 (p53 mutant) cells were treated with 8 Gy RT and TRAIL (1,000 ng/ml) alone or in combination, and cell death was assessed by MTS assay 42 hr posttreatment. The data shown (mean ± SD) is from at least three independent experiments.

we investigated the expression of the TRAIL receptors DR4 and DR5. Previous studies have shown that ionizing radiation can up-regulate DR5 mRNA in a p53-dependent fashion (35). Here we show that DR5 protein expression in MCF7 cells increases markedly, from almost undetectable levels, after radiation treatment (Fig. 3*A*). By contrast, DR4 protein expression remains constant postradiation treatment (Fig. 3*A*).

In further investigations, we took advantage of an MCF7 cell line that stably expresses a dominant negative version of p53 (p53DN) (31). As predicted, the vector control MCF7 cells (p53wt) demonstrated significant synergistic apoptotic activity in response to TRAIL and radiation (Fig. 3*B*). The p53DN-expressing cell line, however, did not show any combined effects (Fig. 3*B*). Consistent with this, we observed up-regulation of the DR5 protein in the p53 wild-type cell line but not in the p53DN cell line (Fig. 3*C*). DR4 protein expression remained constant in both cell lines with or without treatment.

Combined Effect of TRAIL and Ionizing Radiation On Breast Cancer Xenografts *in Vivo*.

Having established the apoptotic potential of TRAIL *in vitro*, we next investigated its tumoricidal activity *in vivo*. MCF7 cell xenografts were established in the mammary fat pad of NIH III nude mice. Treatments were initiated once the tumors had reached a mean volume of 150 mm³. Mice were injected with saline or soluble TRAIL (5 mg/kg) intraperitoneally for 7 days either alone or in combination with radiotherapy. Radiation was delivered in three fractions of 5 Gy each that were administered on days 1, 3, and 5 of the experiment. In
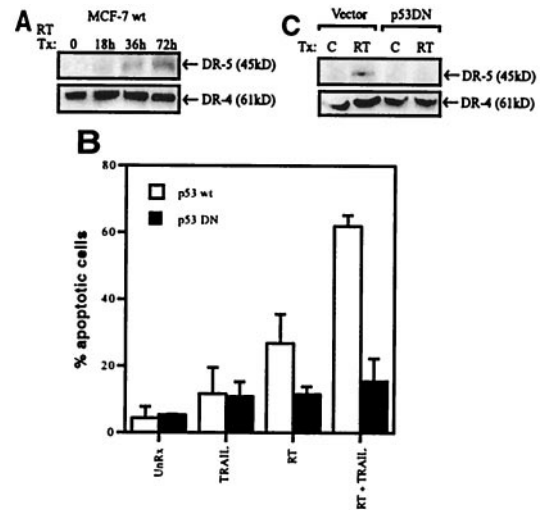

Fig. 3. The synergistic interaction of TRAIL and radiation is p53-dependent and likely is mediated by up-regulation of the DR5 protein (TRAIL receptor). (*A*) Lysates were generated from parental MCF7 cells (p53 wild-type) treated with 8 Gy RT (radiotherapy) and harvested 0, 18, 36, and 72 hr later. After SDS/PAGE, samples were immunoblotted by using a polyclonal antibody directed toward DR4 and DR5. (*B*) MCF7 vector control cells (p53 wild-type) and MCF7 p53DN (dominant negative) expressing cells were treated with 5 Gy RT (radiotherapy) and TRAIL (1,000 ng/ml) alone or in combination and were harvested 24 hr later. Apoptosis was assessed 24 hr later by morphology (DNA staining). The data shown (mean ± SD) is from at least three independent experiments. (*C*) MCF7 vector control cells and MCF7 p53DN cells were treated with 5 Gy RT, and, 24 hr posttreatment, lysates were subjected to immunoblotting with anti-DR4 and anti-DR5 antibodies.

saline-injected mice, the mean tumor volume increased 450% within 15 days after treatment (Fig. 4*A*). In animals treated with TRAIL or radiotherapy alone, mean tumor volumes increased ≈150 and 70%, respectively. By contrast, when TRAIL and radiation were combined, the tumors actually regressed >50% in the same time period (Fig. 4*A*). Tumor volumes were determined 2–3 times a week for over 4 weeks (Fig. 4*B*).

TRAIL and Ionizing Radiation Induced Apoptosis of Breast Cancer Xenografts Monitored By Diffusion MRI.

The therapeutic potential of TRAIL and radiation therapy was monitored in mice by using
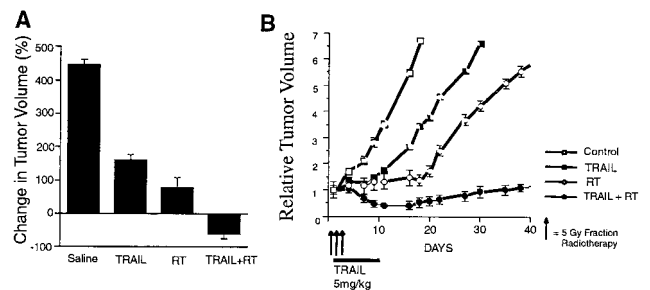

Fig. 4. TRAIL and radiotherapy, in combination, induce regression and slow the growth of breast cancer xenografts. NIH III nude mice harboring MCF7 xenograft tumors were treated with saline, TRAIL (5 mg/kg for 7 days), RT (radiotherapy, three 5-Gy fractions), or a combination of TRAIL and RT. Mean tumor volumes were calculated 15 days after the start of treatment and are expressed as a percent change in tumor volume (*A*). Similarly, mean tumor volumes were assessed 2–3 times a week for over 4 weeks and are expressed in relation to the starting tumor volume (*B*). Six to ten xenografts were used in each experiment, and the data shown is derived from the mean volume ± SEM.
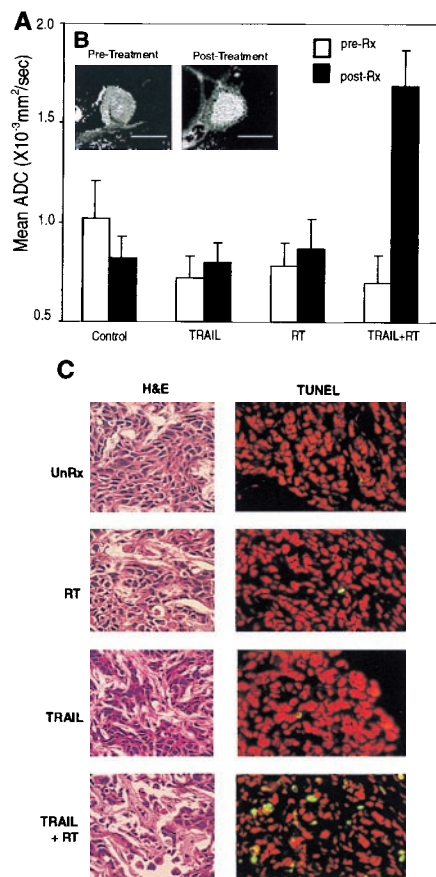
Chinnaiyan et al.

MEDICAL SCIENCES

Fig. 5. Noninvasive imaging of TRAIL- and radiation-induced apoptosis activity as monitored by diffusion MRI. (*A*) Serial histograms of ADC values in control and treated tumors. Mice were imaged at day 0 and 7 days after start of various treatments. The bar graphs displayed are the mean ADC value across pixels within region of interests defined on a representative animal from each treatment or control group. Region-of-interest areas were drawn over three consecutive MR slices near the rim of the respective images for each tumor studied. Graphed are the mean ± SD of ADC values for the regions of interest within a given tumor. (*B*) Isotropic ADC images of a representative tumor before and after TRAIL and radiation treatment. Pixel intensity is directly proportional to the measured ADC. There is a noticeable increase in water mobility after radiation- and TRAIL-combined treatment. Such an increase was not observed in the control or when the treatments were used individually (data not shown). (*C*) Imaged tumors were then assessed for apoptosis. Tumors were sectioned and subsequently stained with hematoxylin and eosin (H&E) or TUNEL. TUNEL-positive cells stain green. Nuclei are counterstained red with propidium iodide.

diffusion-weighted MRI, a sensitive technique that can detect changes in the mobility of extracellular water. Mean ADC of tumors from an animal in each group are summarized in the bar graph shown in Fig. 5*A*. Tumors from control, TRAIL-, or radiation-treated mice did not show significant diffusional changes 7 days after treatment. However, when mice were treated with TRAIL and radiation combined, tumor mean ADC increased markedly, from 0.70 to 1.70 × 10^{-3}/s (Fig. 5*A*). Representative ADC maps of an MCF7 tumor in a mouse before and after treatment with TRAIL and radiation are shown in Fig. 5*B*. An elevation in tumor diffusion was clearly evident on day 7 as increased intensity after initiating combined treatment.

To correlate diffusional changes with apoptosis *in vivo*, tumors that were imaged by diffusion MRI were subsequently sectioned for pathologic analysis. Hematoxylin- and eosin-stained tumor sections showed marked increase in the frequency of apoptotic figures in combined TRAIL- and radiation-treated mice, but not

in the control or single treatment regimens (Fig. 5*C*). Additionally, a loss in cellularity in the combined treatment regimen was observed, indicating treatment efficacy. Furthermore, tissue sections were analyzed by a modified TUNEL assay, which detects 3′ DNA strand breaks, a biochemical hallmark of apoptosis. As predicted, tumors from mice treated with TRAIL and radiation exhibited numerous TUNEL-positive cells as compared with treatment with either agent alone or in control animals (Fig. 5*C*).

Discussion

Among women in the United States, breast cancer is the most prevalent cancer and the second most common cause of cancer death. Estimates suggest that one in nine women will develop breast cancer in her lifetime, about one-third of whom will die from it (36). An improved understanding of the biology of breast cancer has led to the identification of novel therapeutic targets. For example, ≈30% of breast cancers overexpress the HER2/neu oncogene (37), and these tumors are especially aggressive and resistant to chemotherapy. Monoclonal antibodies directed toward HER2 have been shown to regress HER2-overexpressing breast cancers in human trials. Combining anti-HER2 antibody with chemotherapy tripled the response rate and increased overall survival as compared with those receiving chemotherapy alone (38).

In this study, we combine radiation, a common treatment for breast cancer, as well as many other cancers, with the anti-cancer biologic agent TRAIL. The synergistic interaction between TRAIL and radiation is likely mediated by radiation-induced up-regulation of a TRAIL receptor. In addition to proposing a combined therapy, we also investigated the possibility of monitoring apoptosis-inducing anticancer therapies using noninvasive modalities.

TRAIL is an apoptosis-inducing TNF family member and is the most promising candidate as an anticancer therapeutic. TNF and CD95L were the first to be shown to have apoptotic activity against cancer cells; however, subsequent studies revealed significant toxicities. TRAIL, on the other hand, is nontoxic in mice (18) and in primates (24). Although a breadth of cancer cell lines are sensitive to TRAIL, normal cells are remarkably resistant (24). The molecular basis for this difference is controversial and unresolved. Some have proposed that expression of decoy receptors, molecules that bind TRAIL but fail to signal death, may confer resistance to normal tissues. Others have suggested that levels of the intracellular caspase/apoptosis inhibitor FLIP may provide resistance in normal cells (39). Further studies would need to be pursued to clarify this phenomenon.

Previous studies have shown that a mammalian expressed leucine zipper version of TRAIL is nontoxic *in vivo* (18). Similarly, we show that a bacterially generated polyhistidine-tagged version of TRAIL is nontoxic and forms active multimers. A panel of human breast carcinoma cells were assessed for sensitivity to TRAIL. The SUM cell lines tested were recently isolated from breast cancer patients, grown under well defined conditions, and passaged a limited number of times. These cell lines may more accurately reflect breast cancer tumors in patients. Future studies will address the molecular determinants responsible for resistance and sensitivity to TRAIL-induced apoptosis in these cell lines.

The interaction of TRAIL and radiation was initially studied in the MCF7 cell line because these cells are only marginally sensitive to apoptosis induced by TRAIL alone. In MCF7 cells, TRAIL and radiation had a significant apoptotic synergy in response to combined treatment. A similar combined activity was seen in other p53 wild-type breast carcinoma cell lines tested. The p53 negative cell lines, however, failed to exhibit a combined effect. This suggested that p53, a central regulator of growth arrest and apoptosis, may mediate the synergistic interaction

between radiation and TRAIL. A number of studies have used a dominant negative version of p53 to determine its function (40–43), and thus we used an MCF7 cell line that expresses a dominant negative version of p53 (31). This cell line, unlike the matched vector control cell line, failed to exhibit a combined effect with TRAIL and radiation, intimating a significant role for p53 in this process. One mechanism to explain this synergy was suggested by the observation that p53 up-regulates mRNA expression of the DR5 receptor (35). In this study, we demonstrate that radiation up-regulates expression of the DR5 protein, but not the DR4 protein. By expressing more of the TRAIL receptor, cells may then become sensitive to TRAIL. Alternatively, TRAIL and radiation may activate distinct apoptotic programs, which, when jointly triggered, manifest as an amplified response. For example, TRAIL may function to directly activate caspases via its death receptor whereas radiation may preferentially target mitochondria as its mode of apoptosis activation. Triggering both pathways simultaneously may result in the synergistic therapeutic response seen *in vivo*.

Recent studies have demonstrated that systemic TRAIL inhibits the growth of breast and colon cancer xenografts in mice (18, 24). Here we have shown that radiation can enhance the efficacy of TRAIL-induced apoptosis both *in vitro* and *in vivo*. Significantly, the combination of TRAIL and radiation can induce the regression of established tumors, which is distinct from TRAIL's ability to slow growth of tumors, as shown previously.

In clinical oncology and experimental therapies, changes in tumor growth rate or volume are usually the first indication of treatment success. These changes occur late in the course of therapy. The discovery of an early indicator of treatment response would be of great value for experimental and clinical trials, particularly of promising, multistage interventions or combination treatments. In addition, noninvasive assays allow for early characterization of the cellular response to apoptosis-inducing therapies and facilitate the development and optimization of therapeutic dosing schedules. Such an early surrogate marker of therapeutic outcome could also assist to tailor treatments to individual patients. Here we use diffusion-weighted MRI to detect cellularity changes in response to TRAIL and radiation and assess this technique to quantitate therapeutic efficacy *in vivo*. Increased extracellular mobility correlated well with morphologic and biochemical characteristics of apoptosis. In regards to patient care, it may be possible to test a treatment or combination treatment rapidly and adjust the therapeutic protocol according to efficacies determined on an individual basis. Diffusion MRI of tumors may be a useful approach for evaluating emerging anticancer therapies such as TRAIL (which will soon enter clinical trials in humans) and combination regimens such as TRAIL and radiotherapy.

1. Hortobagyi, G. N. (1998) *N. Engl. J. Med.* **339,** 974–984.
2. Hall, E. (1988) *Radiobiology for the Radiologist* (Lippincott, Philadelphia).
3. Steele, G. G., McMillan, T. J. & Peacock, J. H. (1998) *Int. J. Radiat. Biol.* **56,** 525–537.
4. Bradford, J. S. (1991) *Int. J. Radiat. Oncol. Biol. Phys.* **21,** 1457–1469.
5. Nagata, S. (1997) *Cell* **88,** 355–365.
6. Ashkenazi, A. & Dixit, V. M. (1998) *Science* **281,** 1305–1308.
7. Chinnaiyan, A. M. & Dixit, V. M. (1996) *Semin. Immunol.* **9,** 69–76.
8. Nagata, S. (1994) *Adv. Immunol.* **57,** 129–144.
9. Chinnaiyan, A. M., O'Rourke, K., Tewari, M. & Dixit, V. M. (1995) *Cell* **81,** 505–512.
10. Boldin, M. P., Varfolomeev, E. E., Pancer, Z., Mett, I. L., Camonis, J. H. & Wallach, D. (1995) *J. Biol. Chem.* **270,** 7795–7798.
11. Muzio, M., Chinnaiyan, A. M., Kischkel, K. C., O'Rourke, K., Shevchenko, A., Ni, J., Scaffidi, C., Bretz, J. D., Zhang, M., Gentz, R., *et al.* (1996) *Cell* **85,** 817–827.
12. Boldin, M. P., Goncharov, T. M., Goltsev, Y. V. & Wallach, D. (1996) *Cell* **85,** 803–815.
13. Muzio, M., Stockwell, B. R., Stennicke, H. R., Salvesen, G. S. & Dixit, V. M. (1998) *J. Biol. Chem.* **273,** 2926–2930.
14. Pan, G., Ni, J., Wei, Y.-F., Yu, G.-L., Gentz, R. & Dixit, V. M. (1997) *Science* **277,** 815–818.
15. Sheridan, J. P., Marsters, S. A., Pitti, R. M., Gurney, A., Skubatch, M., Baldwin, D., Ramakrishnan, L., Gray, C. L., Baker, K., Wood, W. I., *et al.* (1997) *Science* **277,** 818–821.
16. Pan, G., Ni, J., Yu, G., Wei, Y. & Dixit, V. M. (1998) *FEBS Lett.* **424,** 41–45.
17. Marsters, S. A., Sheridan, J. P., Pitti, R. M., Huang, A., Skubatch, M., Baldwin, D., Yuan, J., Gurney, A., Goddard, A. D., Godowski, P. & Ashkenazi, A. (1997) *Curr. Biol.* **7,** 1003–1006.
18. Walczak, H., Miller, R. E., Ariail, K., Glinak, B., Griffith, T. S., Kibin, M., Chin, W., Jones, J., Woodward, A., Le, T., *et al.* (1999) *Nat. Med.* **5,** 157–163.
19. Ashkenazi, A. & Dixit, V. M. (1999) *Curr. Opin. in Cell Biol.* **11,** 255–260.
20. Tartaglia, L. A. & Goeddel, D. V. (1992) *Immunol. Today* **13,** 151–153.
21. Havell, E. A., Fiers, W. & North, R. J. (1988) *J. Exp. Med.* **167,** 1067–1085.
22. Ni, R., Tomita, Y., Matsuda, K., Ichihara, A., Ishimura, K., Ogasawara, J. & Nagata, S. (1994) *Exp. Cell Res.* **215,** 332–337.
23. Ogasawara, J., Watanabe-Fukunaga, R., Adachi, M., Matsuzawa, A., Kasugai, T., Kitamura, Y., Itoh, N., Suda, T. & Nagata, S. (1993) *Nature (London)* **364,** 806–809.
24. Ashkenazi, A., Pai, R. C., Fong, S., Leung, S., Lawrence, D. A., Marsters, S. A., Blackie, C., Chang, L., McMurtrey, A. E., Hebert, A., *et al.* (1999) *J. Clin. Invest.* **104,** 155–162.
25. Wickelgren, I. (1999) *Science* **285,** 998–1001.
26. Mauceri, H. J., Hanna, N. N., Beckett, M. A., Gorski, D. H., Staba, M. J., Stellato, K. A., Bigelow, K., Heimann, R., Gately, S., Dhanabal, M., *et al.* (1998) *Nature (London)* **394,** 287–291.
27. Galons, J.-P., Altbach, M. I., Paine-Murrieta, G. D., Taylor, C. W. & Gillies, R. J. (1999) *Neoplasia* **1,** 113–117.
28. Pan, G., O'Rourke, K., Chinnaiyan, A. M., Gentz, R., Ebner, R., Ni, J. & Dixit, V. M. (1997) *Science* **276,** 111–113.
29. Liu, S., Tobias, R., McClure, S., Styba, G., Shi, Q. & Jackowski, G. (1997) *Clin. Biochem.* **30,** 455–463.
30. Aida, Y. & Pabst, M. J. (1990) *J. Immunol. Methods* **132,** 191–195.
31. Haldar, S., Negrini, M., Monne, M., Sabbioni, S. & Croce, C. M. (1994) *Cancer Res.* **54,** 2095–2097.
32. Chinnaiyan, A. M., Tepper, C. G., Seldin, M. F., O'Rourke, K., Kischkel, F. C., Hellbardt, S., Krammer, P. H., Peter, M. E. & Dixit, V. M. (1996) *J. Biol. Chem.* **271,** 4961–4965.
33. Rehemtulla, A., Hamilton, C. A., Chinnaiyan, A. M. & Dixit, V. M. (1997) *J. Biol. Chem.* **272,** 25783–25786.
34. Wong, E. C., Cox, R. W. & Song, A. W. (1995) *Magn. Reson. Med.* **34,** 139–143.
35. Sheikh, M. S., Burns, T. F., Huang, Y., Wu, G. S., Amundson, S., Brooks, K. S., Fornace, A. J., Jr. & el-Deiry, W. S. (1998) *Cancer Res.* **58,** 1593–1598.
36. Fishman, M., Hoffman, A., Klausner, R. & Thaler, M. (1991) *Medicine* (Lippincott, Philadelphia).
37. Slamon, D. J., Clark, G. M., Wong, S. G., Levin, W. J., Ullrich, A. & McGuire, W. L. (1987) *Science* **235,** 177–182.
38. Slamon, D. J. & Clark, G. M. (1988) *Science* **240,** 1795–1798.
39. Griffith, T. S., Chin, W. A., Jackson, G. C., Lynch, D. H. & Kubin, M. Z. (1998) *J. Immunol.* **161,** 2833–2840.
40. Nair, P., Muthukkumar, S., Sells, S. F., Han, S. S., Sukhatme, V. P. & Rangnekar, V. M. (1997) *J. Biol. Chem.* **272,** 20131–20138.
41. Gao, Q., Hauser, S. H., Liu, X. L., Wazer, D. E., Madoc-Jones, H. & Band, V. (1996) *Cancer Res.* **56,** 3129–3133.
42. Hachiya, M., Chumakov, A., Miller, C. W., Akashi, M., Said, J. & Koeffler, H. P. (1994) *Anticancer Res.* **14,** 1853–1859.
43. Shaulian, E., Zauberman, A., Ginsberg, D. & Oren, M. (1992) *Mol. Cell. Biol.* **12,** 5581–5592.

MEDICAL SCIENCES

Chinnaiyan et al.

www.manaraa.com